

**Carbon nanotube-linked hollow carbon nanospheres doped with iron and nitrogen as single-atom catalysts for oxygen reduction reaction in acidic solutions**

Jin-Cheng Li,<sup>a, b, c</sup> Min Cheng,<sup>c</sup> Tao Li,<sup>d, e</sup> Lu Ma,<sup>d</sup> Xiaofan Ruan,<sup>b</sup> Dong Liu,<sup>b</sup> Hui-Ming Cheng,<sup>c</sup> Chang Liu,<sup>\*c</sup> Dan Du,<sup>b</sup> Zidong Wei,<sup>f</sup> Yuehe Lin <sup>\*b</sup> and Minhua Shao <sup>\*a, g</sup>

<sup>a</sup> Fok Ying Tung Research Institute, Hong Kong University of Science and Technology, Guangzhou 511458, China.

<sup>b</sup> School of Mechanical and Materials Engineering, Washington State University, Pullman, WA 99164, USA.

<sup>c</sup> Shenyang National Laboratory for Materials Science, Institute of Metal Research, Chinese Academy of Sciences, Shenyang 110016, China.

<sup>d</sup> Department of Chemistry and Biochemistry, Northern Illinois University, 1425 W. Lincoln Hwy., DeKalb, IL, 60115, USA.

<sup>e</sup> X-ray Science Division, Argonne National Laboratory, 9700 South Cass Avenue, Lemont, Illinois 60439, United States.

<sup>f</sup> College of Chemistry and Chemical Engineering, Chongqing University, Chongqing, 400044, China

<sup>g</sup> Department of Chemical and Biological Engineering, Hong Kong University of Science and Technology, Clear Water Bay, Kowloon, Hong Kong, China.

\*E-mail: [cliu@imr.ac.cn](mailto:cliu@imr.ac.cn) (C. Liu), [yuehe.lin@wsu.edu](mailto:yuehe.lin@wsu.edu) (Y. Lin), or [kemshao@ust.hk](mailto:kemshao@ust.hk)

(M. Shao)

## **Experimental methods**

### **1. Material preparation**

#### *1.1. Preparation of functionalized CNTs*

3 g carbon nanotubes (nominal outsider diameter: < 8 nm, Nanografi Nano Technology) were added into a mixture solution (400 ml) of concentrated nitric acid and concentrated sulfuric acid with a volume ratio of 1:3 under vigorous stirring in an oil bath at 80 °C. After stirring for 2 h, the mixture solution was cooled down to room temperature and was then centrifuged at 8000 rpm for 5 min. The CNTs in sediment were collected using a vacuum filter and washed with deionized water and dried for use.

#### *1.2. Preparation of CNT-Fe/NHCNS*

0.15 g polyvinyl pyrrolidone (PVP, 40 k) was dissolved in 30 ml deionized water. Then 0.15 g functionalized CNTs were added into the PVP solution. After an ultrasonic treatment about 1 hour, 0.7 ml aniline and 0.5 ml pyrrole were added into the above mixture under continuous stirring in an ice bath. 2.0 g ammonium peroxydisulfate (APS) solution was then added to polymerize the aniline and pyrrole. After stirring for 24 h to allow for polymerization, the product (CNT-linked polymer nanospheres) was separated by vacuum filtration and washed with ethanol and water. The wet composition was then dispersed in 100 ml of a mixture of sodium chloride (0.4 M) and iron nitrate (0.02 M), followed by 2 min of sonication and 24 h of

vigorous stirring to allow it to adsorb  $\text{Na}^+$  and  $\text{Fe}^{3+}$  cations. This hybrid precursor was collected by vacuum filtration and dried at 60 °C for 12 h and pyrolyzed at 900 °C under a  $\text{N}_2$  atmosphere for 30 min. The obtained carbon material was soaked in with a 0.5 M  $\text{H}_2\text{SO}_4$  solution at 60 °C for 4 h to remove  $\text{NaCl}$  and unstable Fe species and then annealed at 900 °C under  $\text{NH}_3$  atmosphere for 30 min to obtain the final CNT-Fe/NHCNS catalyst.

## **2. Material characterization**

The carbon-based materials were characterized using scanning electron microscopy (SEM, Nova NanoSEM 430, operated at 15 kV; FEI Sirion 200, operated at 30 kV), transmission electron microscopy (TEM, Philips CM200 UT, 200 kV; Hitachi HD2700, 200 kV), Raman spectroscopy (Jobin Yvon HR800), X-ray photoelectron spectroscopy (XPS, Escalab 250, Al  $\text{K}\alpha$ ), X-ray diffraction (XRD, Rigaku Miniflex 600, 40 kV), inductively coupled plasma mass spectrometry (ICP-MS, Perkin Elmer Optima 4300 DV), and thermogravimetric analysis (NETZSCH STA 449C). The specific surface area and pore structure of the samples were investigated with an automatic volumetric sorption analyzer (ASAP 2020 M) using  $\text{N}_2$  as the adsorbate at -196 °C..

The X-ray absorption spectroscopy measurement at Fe K-edge was performed at the Advanced Photon Source (APS) on the bending-magnet beamline 9-BM-B with electron energy of 7 GeV and average current of 100 mA. The radiation was monochromatized by a Si (111) double-crystal monochromator. Harmonic rejection was accomplished with Harmonic rejection mirror. All spectra were collected in

fluorescence mode by vortex four-element silicon drift detector. XAS data reduction and analysis were processed by Athena software.

### 3. Electrochemical measurements

The electrochemical measurements were performed using a standard three-electrode cell. A graphite rod and a calomel electrode filled with saturated KCl aqueous solution served as the counter electrode and reference electrode, respectively. All potential values refer to that of a reversible hydrogen electrode (RHE). To prepare the working electrode, 5.0 mg of the catalyst was ultrasonically dispersed in an ethanol solution containing 0.05 wt% Nafion (1.0 ml) to form a dispersion of 5.0 mg/ml catalyst. This catalyst dispersion was then coated on the surface of a glassy carbon disk for the ORR tests. The noble-free catalyst loading for the ORR tests was  $0.2 \text{ mg cm}^{-2}$  in 0.1 M HClO<sub>4</sub> solution. Commercial Pt/C catalyst (20 wt.% of Pt, Alfa Aesar) with a standard loading of  $0.1 \text{ mg cm}^{-2}$  was used as a benchmark. RDE and RRDE measurements were performed in O<sub>2</sub>-saturated 0.1 M HClO<sub>4</sub>. The scan rate was 5 mV/s. To avoid the effect of capacitance of noble-metal-free catalysts on the ORR performance evaluation, background currents recorded in a N<sub>2</sub>-saturated 0.1 M HClO<sub>4</sub> solution were deducted. Cyclic voltammetry (CV) in N<sub>2</sub>-saturated 0.1 M HClO<sub>4</sub> electrolyte at a scan rate of 20 mV/s to calculate the electrochemically accessible surface area ( $S_a$ ). The effective  $S_a$  (m<sup>2</sup>/g) can be deduced from the gravimetric double layer capacitance  $C$  (F/g) according to the following formula:

$$S_a = \frac{C}{C_{GC}} = \frac{\int_{V_a}^{V_b} I(V) dV}{m * v * C_{GC}}$$

where  $I(V)$  is the current,  $V_a$  is the low potential,  $V_b$  is the high potential,  $m$  is the

catalyst mass on glassy carbon (GC) electrode,  $\nu$  is the scan rate, and  $C_{GC}$  is the double layer capacitance of glassy carbon electrode surface (0.2 F/m<sup>2</sup>). RDE polarization curves were collected at disk rotation rates of 400, 800, 1200, 1600, and 2000 rpm. The electrons transfer number ( $n$ ) was calculated on the basis of the Koutecky–Levich equation:

$$\frac{1}{J} = \frac{1}{J_L} + \frac{1}{J_K} = \frac{1}{B\omega^{1/2}} + \frac{1}{J_K}$$

$$B = 0.62nFC_0(D_0)^{2/3}\nu^{-1/6}$$

$$J_K = \frac{1}{nkFC_0}$$

$J$  is the measured current density,  $J_K$  and  $J_L$  are the kinetic- and diffusion-limiting current densities,  $\omega$  is the angular velocity,  $F$  is the Faraday constant ( $F = 96500$  C/mol),  $C_0$  is the bulk concentration of O<sub>2</sub> in the electrolyte ( $C_0 = 1.26 \times 10^{-6}$  mol/cm<sup>3</sup>),  $D_0$  is the diffusion coefficient of O<sub>2</sub> in the electrolyte ( $D_0 = 1.93 \times 10^{-5}$  cm<sup>2</sup>/s),  $\nu$  is the kinematic viscosity of the electrolyte ( $\nu = 1.009 \times 10^{-2}$  cm<sup>2</sup>/s), and  $k$  is the electron-transfer rate constant.

RRDE Polarization curves were collected at a disk rotation rate of 1600 rpm. The potential of the ring was set at 1.3 V in 0.1 M HClO<sub>4</sub>. The collection efficiency of the RRDE ( $N$ ) was 0.37. The peroxide yield (H<sub>2</sub>O<sub>2</sub>%) and the electron transfer number ( $n$ ) were calculated as follows:

$$H_2O_2 \% = 200 \times \frac{I_r / N}{I_d + I_r / N}$$

$$n = 4 \times \frac{I_d}{I_d + I_r / N}$$

where  $I_d$  is the disk current and  $I_r$  is the ring current.

The accelerated durability test protocol was performed by cycling the catalysts between 0.7 and 1.1 V at 50 mV s<sup>-1</sup>.

Turn-over frequency (TOF, number of electrons reduced per Fe-N-C active site and per second) was calculated according to the following formula:

$$\begin{aligned}
 TOF &= \frac{j_k}{\frac{W_{Fe}}{M_{Fe}} \times N_A \times m_{loading}} \\
 &= \frac{|j_k|(mA \cdot cm^{-2}) \times 10^{-3}(A \cdot mA^{-1})}{\frac{10^{-2} \times |W_{Fe}|(wt. \%)}{55.85(g \cdot mol^{-1})} \times 6.02 \times 10^{23}(site \cdot mol^{-1}) \times 0.2 \times 10^{-3}(g \cdot cm^{-2})} \\
 &= \frac{|j_k|(mA \cdot cm^{-2}) \times 10^{-3}(C \cdot s^{-1} \cdot mA^{-1})}{\frac{10^{-2} \times |W_{Fe}|(wt. \%)}{55.85(g \cdot mol^{-1})} \times 6.02 \times 10^{23}(site \cdot mol^{-1}) \times 0.2 \times 10^{-3}(g \cdot cm^{-2})} \\
 &= \frac{|j_k|(mA \cdot cm^{-2}) \times 10^{-3} \times 6.25 \times 10^{18}(e^- \cdot s^{-1} \cdot mA^{-1})}{\frac{10^{-2} \times |W_{Fe}|(wt. \%)}{55.85(g \cdot mol^{-1})} \times 6.02 \times 10^{23}(site \cdot mol^{-1}) \times 0.2 \times 10^{-3}(g \cdot cm^{-2})} \\
 &= 0.29 \times \frac{|j_k|}{|W_{Fe}|} (e^- \cdot site^{-1} \cdot s^{-1})
 \end{aligned}$$

Where  $W_{Fe}$  and  $M_{Fe}$  ( $|M_{Fe}| = 55.85 \text{ g mol}^{-1}$ ) are the mass fraction and molar mass of Fe, respectively.  $W_{Fe}$  is measured from ICP-MS analysis.  $j_k$  is the mass transfer corrected kinetic current density.  $N_A$  is Avogadro's number ( $6.02 \times 10^{23} \text{ mol}^{-1}$ ).

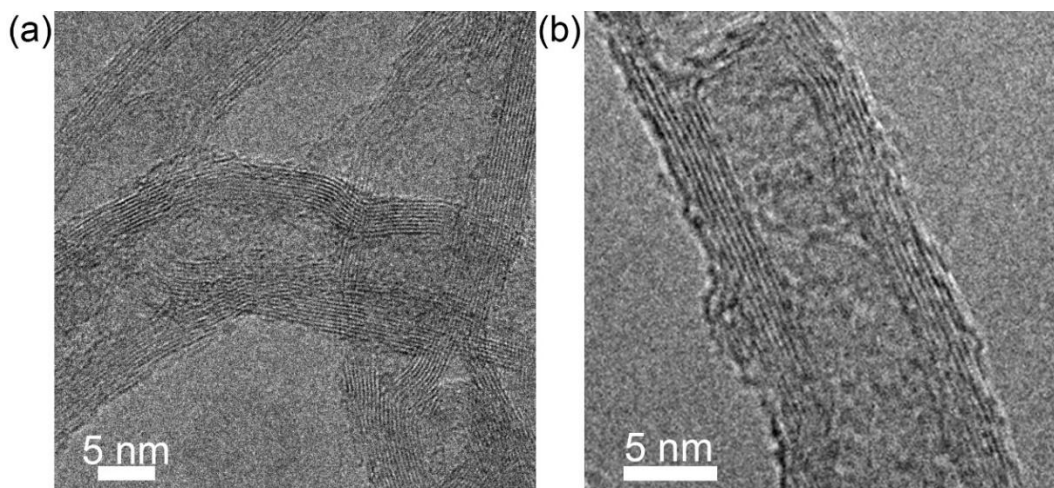


**Figure S1.** TEM images of the functionalized CNTs.

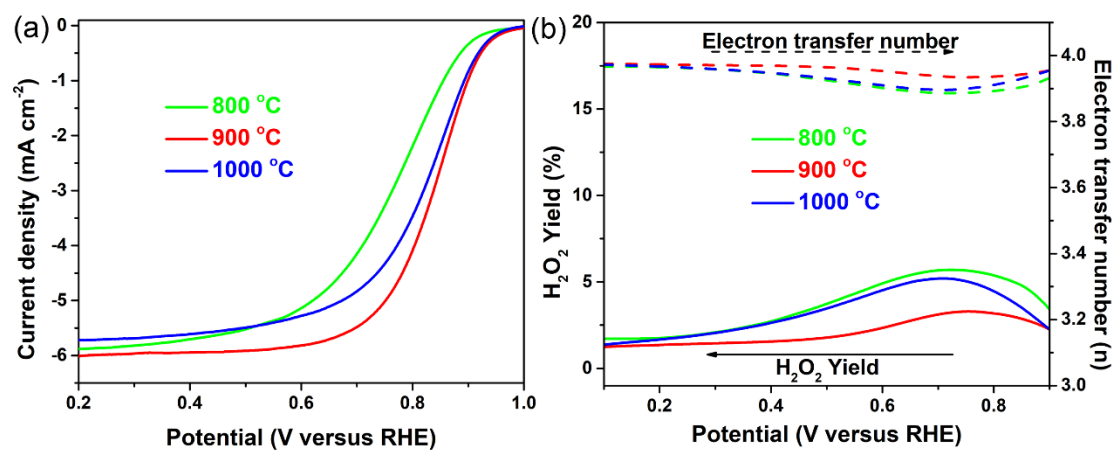


**Figure S2.** (a) ORR polarization curves and (b)  $\text{H}_2\text{O}_2$  yield and electron transfer number of the CNT-Fe/NHCNS samples prepared at different temperatures.

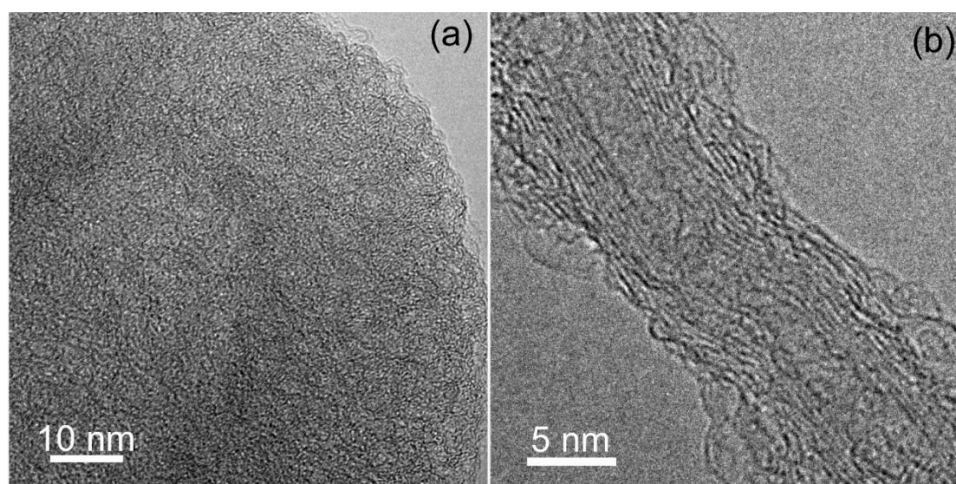


**Figure S3.** HRTEM images of the (a) hollow carbon nanosphere and (b) CNT in the CNT-Fe/NHCNS hybrid.

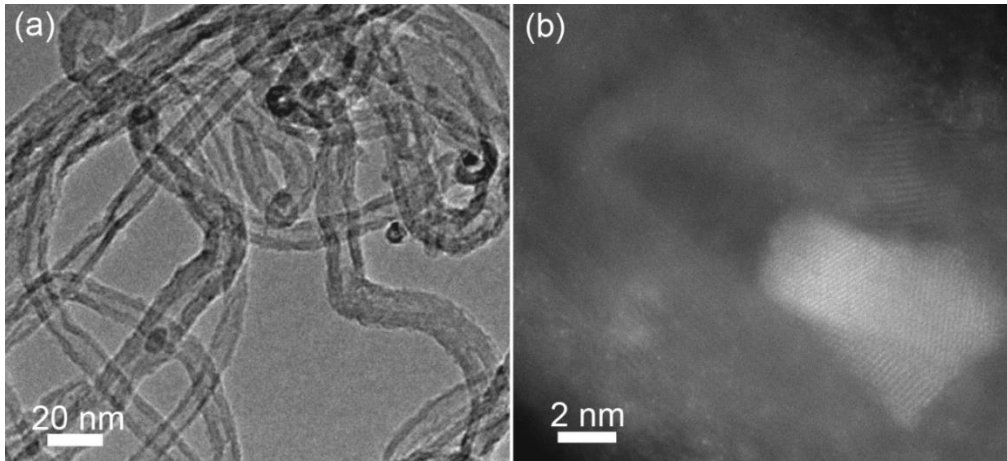


**Figure S4.** (a) TEM images of the functionalized CNTs. (b) ADF-STEM image of CNT-Fe/NHCNS.

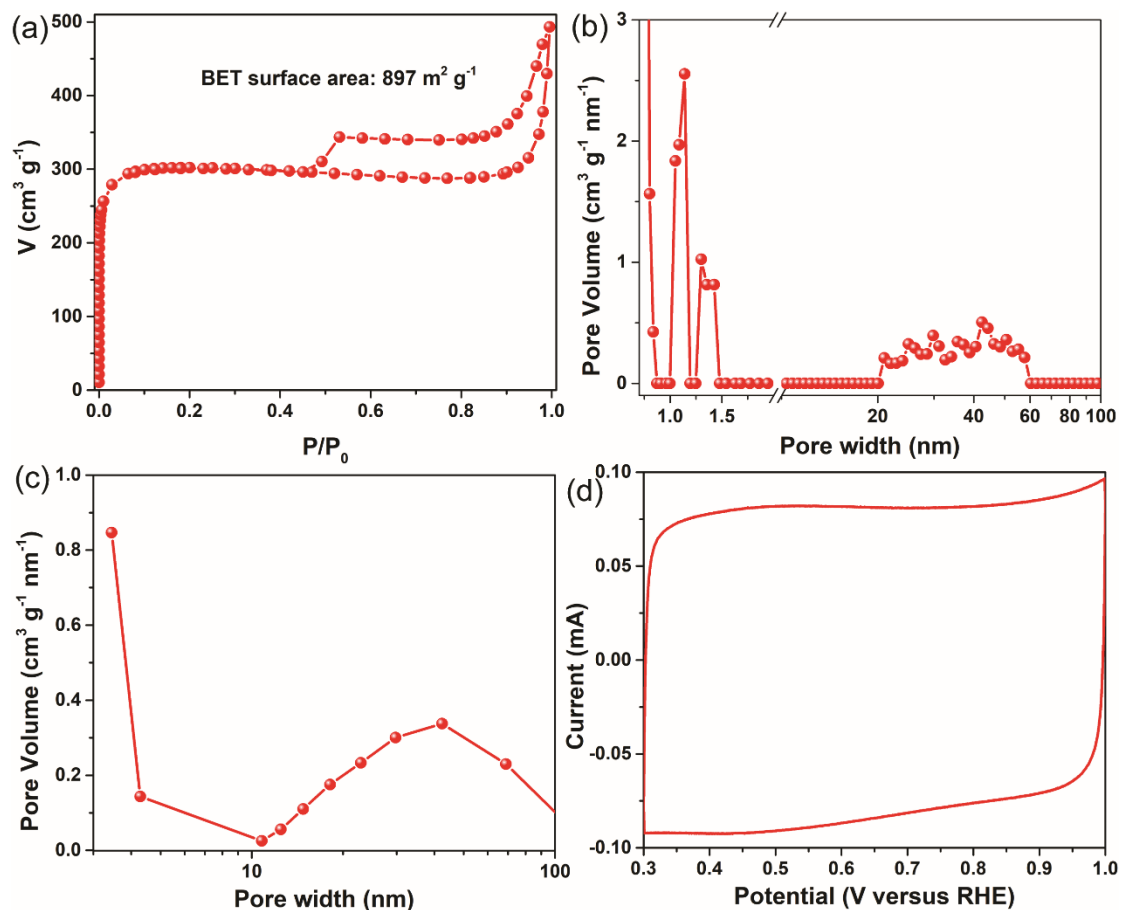


**Figure S5.** (a) Nitrogen adsorption-desorption isotherm curve, pore distribution curve deduced from (b) nonlocal density functional theory and (c) Barrett-Joyner-Halenda model, and (d) CV curve of CNT-Fe/NHCNS.



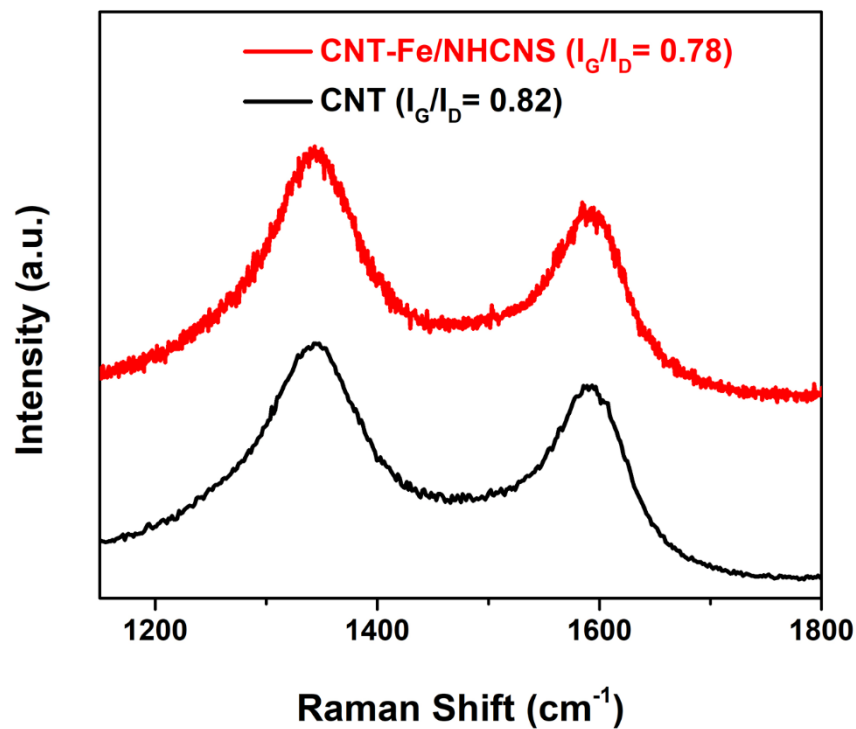


**Figure S6.** Raman spectra of the CNT-Fe/NHCNS and CNT materials.

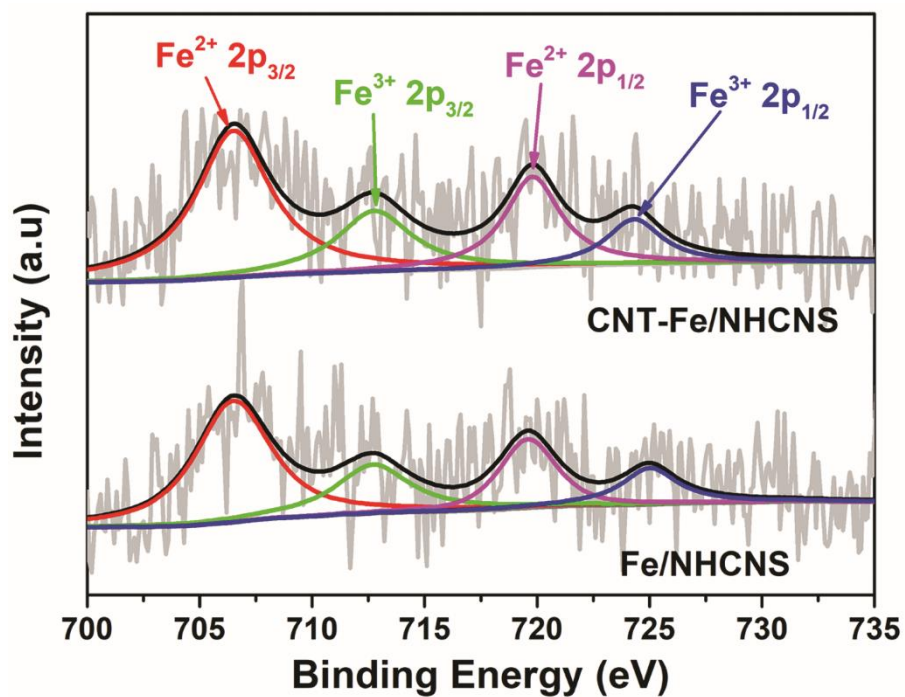


**Figure S7.** High-resolution Fe 2p spectra of CNT-Fe/NHCNS and Fe/NHCNS.

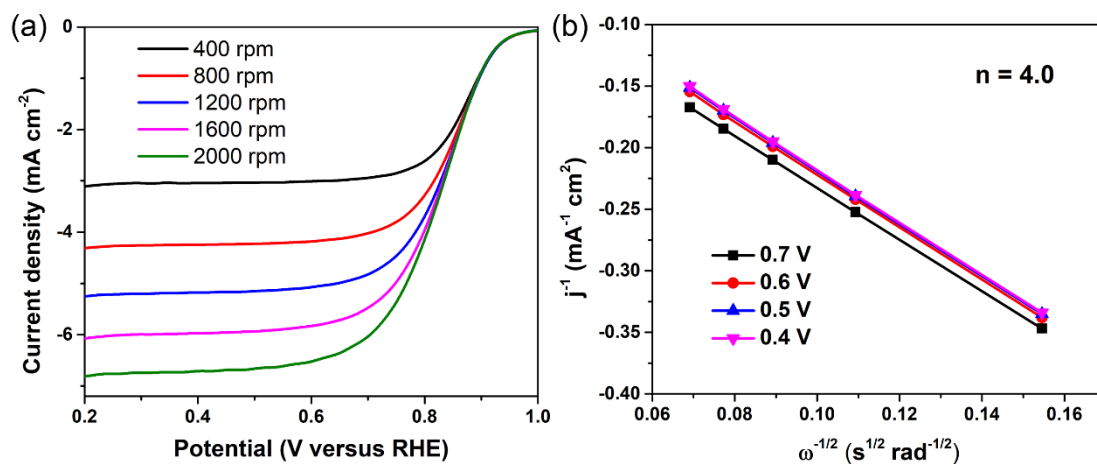


**Figure S8.** (a) RDE voltammograms of CNT-Fe/NHCNS in O<sub>2</sub>-saturated 0.1 M HClO<sub>4</sub> at various rotating speeds. (b) K-L plots at various potentials derived from (a).

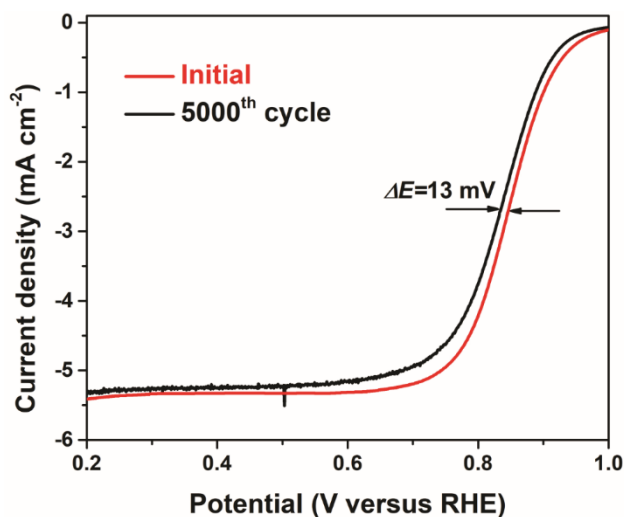


**Figure S9.** ORR polarization curves of Pt/C before and after 5000 potential cycles.

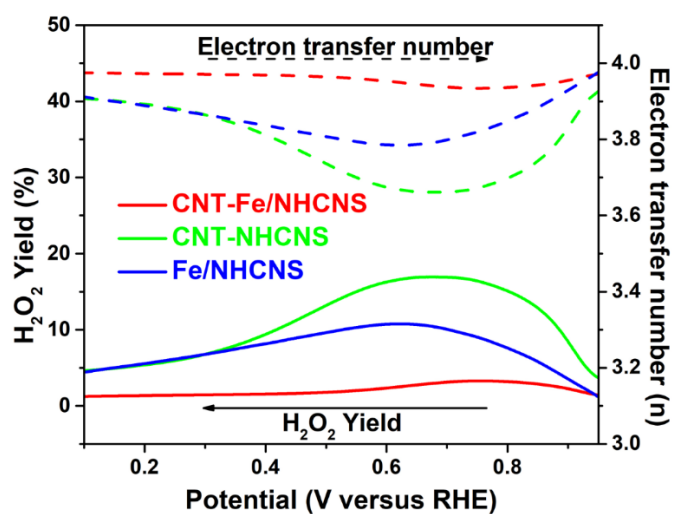


**Figure S10.**  $\text{H}_2\text{O}_2$  yield and electron transfer number of CNT-Fe/NHCNS, CNT-NHCNS, and Fe/NHCNS.

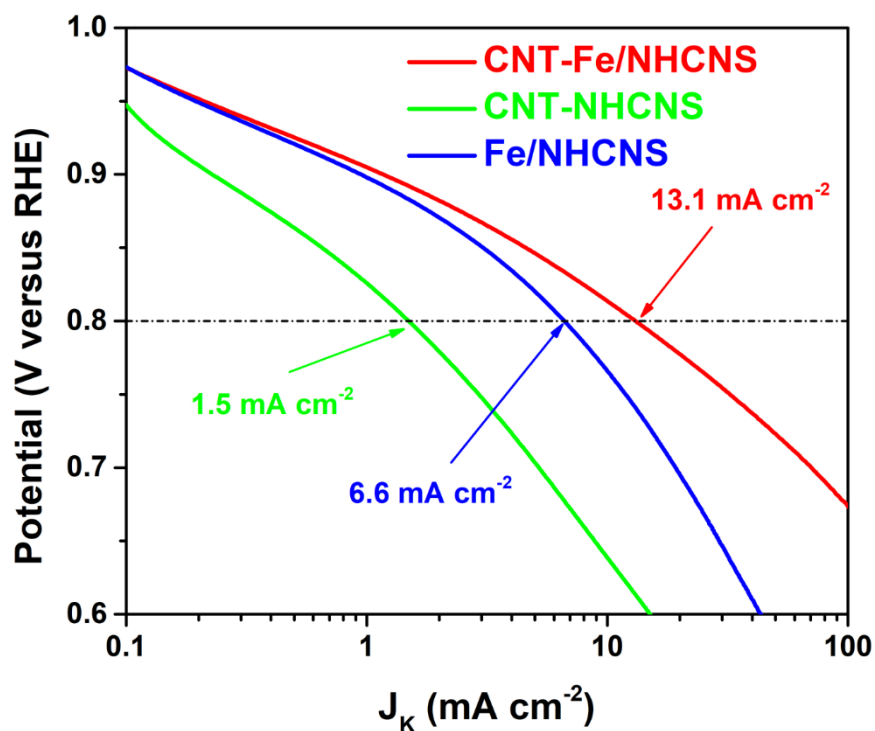


**Figure S11.** Tafel plots of CNT-Fe/NHCNS, CNT-NHCNS, and Fe/NHCNS.

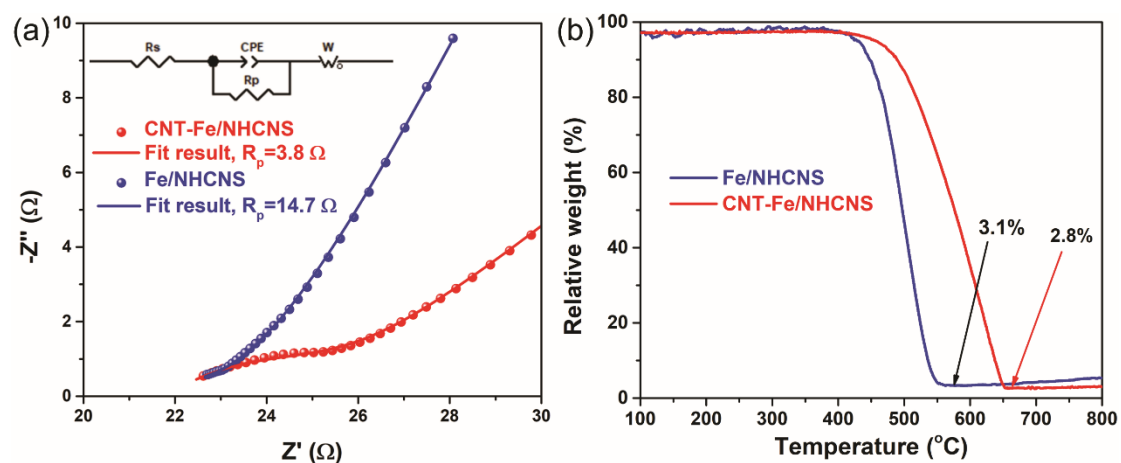


**Figure S12.** (a) Electrochemical impedance spectra and (b) thermogravimetry curves of Fe/NHCNS and CNT-Fe/NHCNS.

**Table S1.** EXAFS data fitting results of Samples.

Sample	Scatter	CN	R (Å)	$\sigma^2$ (Å <sup>2</sup> )	E <sub>0</sub> (eV)
CNT-Fe/NHCNS	Fe-N	4.45±1.23	1.990±0.029	0.0143±0.0048	-3.31

**Table S2.** Comparison of the metal loadings and estimated average turn-over frequencies (TOF) of the catalysts described in this work with those reported previously.

Reference	Material	Fe content (wt.%)	Average TOF at 0.8 V ( $e^- \text{ site}^{-1} \text{ s}^{-1}$ )
<b><i>This work</i></b>	<b>CNT-Fe/NHCNS</b>	<b>2.18</b>	<b>1.74</b>
<i>Nat. Commun.</i> 2015, 6, 8618	Fe-N-C-2HT-2AL (Fe,Mn)-N-C-3HT-2AL	6.0 3.0	0.21 0.34
<i>Nat. Mater.</i> 2015, 14, 937-942	Fe <sub>0.5</sub> Fe <sub>0.5</sub> -900	1.5 1.2	0.06 0.17
<i>Energy Environ. Sci.</i> 2016, 9, 2418-2432	FePhenMOF-ArNH <sub>3</sub>	0.5	0.96